

Swept Wind Turbine Blade Aeroelastic Modeling for Loads and Dynamic Behavior

Scott Larwood
UC Davis
Davis, CA

Mike Zuteck
MDZ Consulting
Clear Lake Shores, TX

ABSTRACT

A dynamic modeling effort of a swept-blade wind turbine rotor has been conducted. The swept-blade concept was used for increased energy capture without an increase in the turbine loads. The work is part of a Department of Energy contract for increased wind energy capture at low-wind speed sites. The blade works by twisting to feather under aerodynamic loads at the outboard region. Conceptual design of the blade resulted in a 28 m blade radius for eventual testing on a normally 50 m diameter turbine. The blade was modeled with codes developed by the National Renewable Energy Laboratory. Comparisons were made to an unswept rotor of the same diameter and a baseline 50-m rotor. The results demonstrated the twisting and load-reduction behavior of the swept rotor. Little detriment in the power curve was shown with the swept blade, and substantial power increase over the 50 m baseline was obtained in below-rated power.

NOMENCLATURE

English Variables:

C_L	=	lift coefficient
$C_{L\Lambda}$	=	lift coefficient adjusted for blade sweep
C_{PO}	=	peak power coefficient
k	=	generator torque control constant, N·m/rpm ²
Q_{gen}	=	generator mechanical torque, N·m
R	=	rotor radius, m

Greek Variables:

λ_O	=	optimum tip-speed ratio
Λ	=	blade sweep angle, radians or degrees
ρ	=	atmospheric density, kg/m ³
ω_{gen}	=	generator rotational speed, rpm

Acronyms:

DOE	=	United States Department of Energy
GL	=	Germanischer Lloyd
IEC	=	International Electrotechnical Commission
LWST	=	Low Wind Speed Technology
NREL	=	National Renewable Energy Laboratory

INTRODUCTION

This paper describes the dynamic analysis of a swept wind-turbine blade concept that was developed under a U.S. Department of Energy (DOE) program. At the time of this writing, the wind power industry had experienced exponential growth in the last decade. The decrease in cost of wind power generation, however, has slowed due to the maturity of the technology. All reductions in the cost of energy were now coming in small increments. In this current engineering climate, the DOE initiated the Low Wind Speed Technology (LWST) program to move research in the direction of capturing more wind energy in low wind speed areas, thus positively affecting the economics for these regions.

One thrust of the LWST program was in advanced rotor control concepts. The main idea was to increase the rotor diameter for a given turbine rating without increasing the load envelope. One concept (Lobitz, Veers et al. 1996) was to incorporate flap/twist coupling into the rotor with off-axis fiber orientation into the blade construction. As the blade deflects in the flapwise direction, the tip would twist towards feather and reduce the aerodynamic loading. A different physical mechanism, leading to similar aerodynamic load reduction, was analyzed by Zuteck (2002) and proposed earlier by Liebst (1986). This concept was to sweep the outboard-region rotor planform in the plane of rotation aft of the pitch axis. The loads generated at the tip would introduce a moment about the pitch axis. With sufficient blade torsional flexibility, the tip would twist towards feather, thus reducing the loads. This concept is illustrated below in Figure 1.

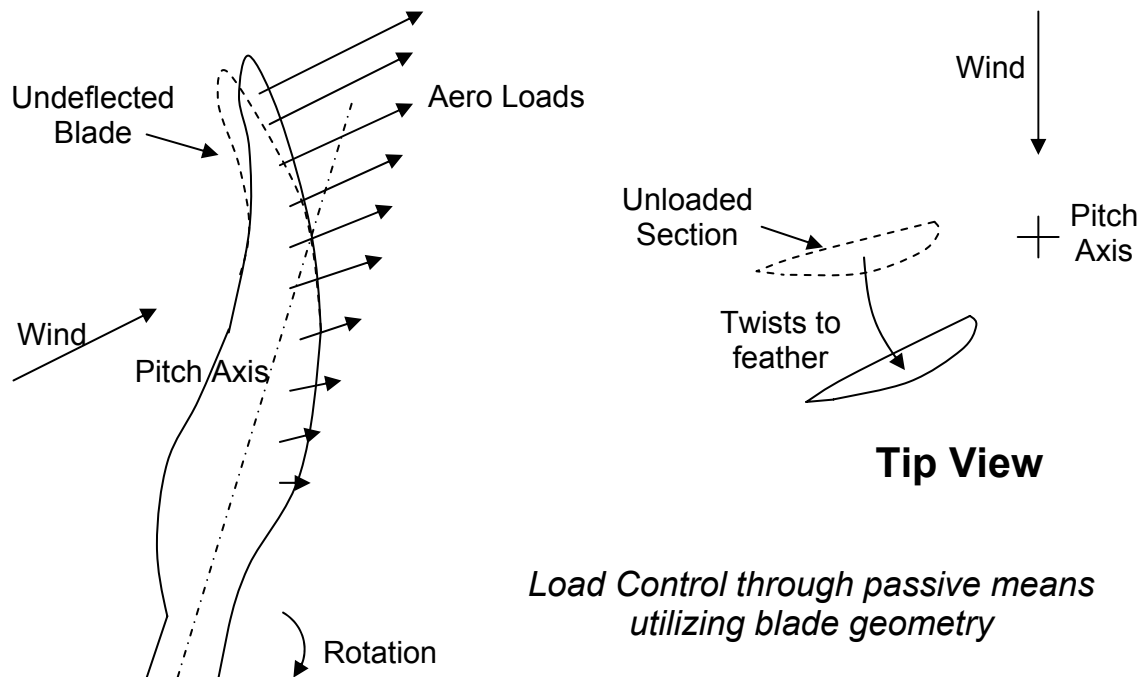


Figure 1. Swept blade concept.

Zuteck outlined key design parameters for the concept that included the sweep-curve geometry and tip sweep. He estimated that 4° to 7° of tip twist would be needed to shed loads for a 30 m blade. This amount of tip twist would require that the torsional stiffness of the blade be decreased in comparison to typical straight-blade designs, but it was shown to be feasible through appropriate design modifications. Liebst had also concluded that the torsional stiffness would have to be reduced for the concept to be successful.

In 2004 the wind turbine blade division of Knight & Carver won a LWST contract administered through Sandia National Labs. Knight and Carver assembled a team to design, manufacture, and test a rotor based on the swept-blade concept. The rotor would be designed for atmospheric testing on a Zond Z-50 wind turbine with 750 kW rating. The rotor was to be designed according to the requirements of the International Electrotechnical Commission (IEC) Class IIA wind regime (IEC-TC88 2005). The authors were responsible for the structural design and analysis of the prototype blade. As will be shown in this paper, a dynamic analysis of the rotor using state-of-the-art tools demonstrated the increased power capture of the rotor while maintaining turbine loads near baseline limits.

METHODS

Conceptual Design

The design goal of the project was to increase annual energy capture of the baseline turbine by 5%-10%. The rotor swept area was increased by 25% to increase the below-rated energy capture by 25% for a straight-bladed rotor. With sweep and twist, it was expected that the increase in below-rated energy capture would be 15%-20% and therefore would increase the overall annual energy capture by 5%-10%. The turbine power rating would not be increased; therefore there would be no expected increase in above-rated energy capture. For the Z-50 turbine, the rotor radius was increased from 25 m to 28 m.

Kevin Jackson of Dynamic Design Engineering, Inc. developed the planform for a 25 m blade as a baseline design case. The 50-year extreme wind loads for the parked rotor were calculated for this baseline with a static load distribution. Swept planforms of 28 m were then designed by maintaining a similar extreme-load root bending moment. Airfoils developed by Wortmann and compiled by Althaus (1986) for wind power application were used. Based on previous investigations comparing straight and swept rotors with a lifting-surface wind turbine analysis code, the lift coefficient (C_L) was modified for sweep using the following relationship:

$$C_{L\Lambda} = C_L \cos^2 \Lambda \quad (1)$$

Where:

$C_{L\Lambda}$ = lift coefficient adjusted for blade sweep
 Λ = blade sweep angle, radians or degrees

This is the same relationship used for modifying the lift coefficients of swept wings (Hoerner 1985). The drag and moment coefficients were not modified.

The maximum sweep at the tip was maintained within the envelope of the maximum chord for transportation considerations. During this process the chord and twist distribution were changed to optimize the peak power coefficient (C_{PO}).

After the aerodynamic planform had been established, the structural design was performed using section analysis techniques. The simplified extreme loads and operating loads were used for this process. It became apparent that the blade would be designed for stiffness for the blade deflection constraints. The section design was performed to maintain the blade deflection to one-half of the allowable clearance under rated operating conditions. This requirement would be validated later in the dynamic analysis, which has a 1.6 safety factor for critical deflections. The section properties were then used as input for the dynamic modeling. In addition, the section properties were later validated with a finite-element model of the blade.

Dynamic Analysis

During the conceptual design we looked at different tools to be used for dynamic analysis. The tools would have to allow sweep in the blade geometry and allow for twist under load. Both Garrad Hassan's Bladed and Stig Øye's Flex5 programs were considered. Under the advice of Craig Hansen at Windward Engineering, we decided to use the newly developed capabilities of FAST (Jonkman and Buhl Jr 2004) as a pre-processor for MSC/ADAMS[®]. These modifications were implemented by the National Renewable Energy Laboratory (NREL). This analysis option was also the lowest cost with ADAMS under an academic license.

A diagram of the dynamic analysis process utilizing FAST with ADAMS is shown below in Figure 2. Turbine system properties, such as airfoil section data, blade structural properties, generator efficiency, etc. are used to build input files for FAST and the aerodynamic subroutines of AeroDyn. For the particular design load case to be studied, the NREL developed programs TurbSim (Kelley and Jonkman 2005) and IECWind (Laino 2005a) are used to develop the input wind fields. FAST is then run to build the large ADAMS datasets. ADAMS is then executed to perform the dynamic calculations. During operation, ADAMS calls the linked AeroDyn subroutines to compute the aerodynamic blade forces. The output of the process is time series files of desired parameters.

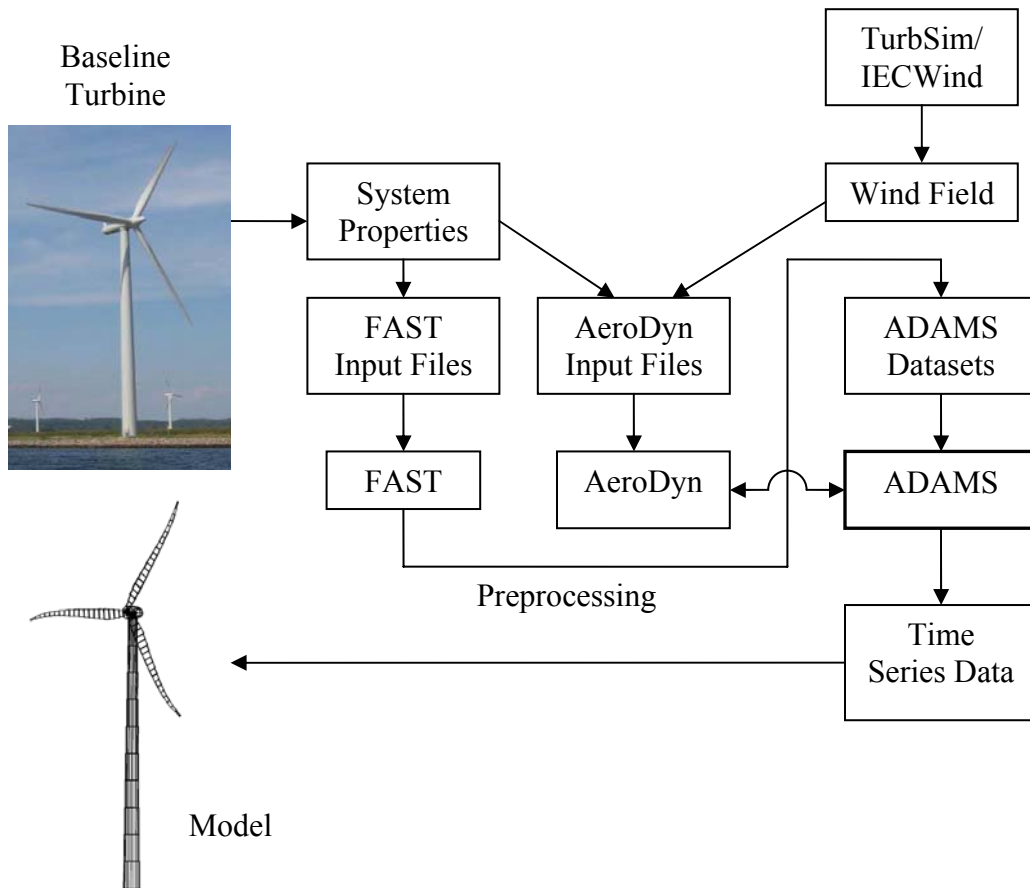


Figure 2. Analysis flow diagram.

Prior to developing the dynamic model, an aerodynamic model was built using the NREL-developed WT_Perf program (Buhl Jr 2005). Peak power coefficients, optimum pitch, and optimum tip-speed ratio were determined from this step. The next step was to run a simplified model in YawDyn (Laino 2005b). A stepped-wind input file was used to develop a power curve to compare to the WT_Perf results. Because YawDyn also uses the AeroDyn subroutines, this process allowed checking of the input files that would be used for FAST/ADAMS.

After this initial checkout phase of the analysis process, ADAMS was run with fixed rotor speed and a uniform wind speed to study the quasi-static twisting behavior of the rotor. A controller was then developed to run the IEC loads cases. The baseline turbine used a standard variable-speed torque controller and with full-span pitch for rotor speed control. The torque controller operated according the formula:

$$Q_{gen} = k\omega_{gen}^2 \quad (2)$$

Where:

Q_{gen} = generator mechanical torque, N·m
 k = generator torque control constant, N·m/rpm²
 ω_{gen} = generator rotational speed, rpm

The generator torque control constant for peak power capture was determined by (Fingersh and Carlin 1998):

$$k = \frac{\rho\pi R^5 C_{PO}}{2\lambda_o^3} \quad (3)$$

Where:

ρ = atmospheric density, kg/m³
 R = rotor radius, m
 λ_o = optimum tip-speed ratio

The torque controller was validated using the stepped wind input and comparing the torque/speed relationship to Eq. (2).

For the pitch controller, the gains from an existing model for the WindPACT 1.5 MW were modified by scaling the gains based on the rotor inertia. This WindPACT model came with the examples files in the FAST download from the NREL website (Jonkman 2005). To verify proper operation of the controller, 1 m/s stepped inputs were simulated at 11 m/s, 14 m/s and 20 m/s. Overshoots in generator rpm and blade pitch were determined acceptable and no stability problems were observed in turbulent simulations. Further optimization of the controller was expected to be conducted in the future according to methods outlined by Hand (1999).

During this modeling phase, we did not have tower or drivetrain characteristics for the Z-50 turbine. We therefore modeled with these degrees of freedom disabled. The full-system rotor modes, and coupled rotor/tower modes are therefore not included in this presentation.

Full wind field turbulent simulations were to be performed for the IEC operating load cases. Details of the turbulence model inputs are shown below in Table 1:

Table 1. Turbulence Model Parameters

Random Number Generator	RANLUX
Vertical grid point dimension	5 m
Horizontal grid point dimension	5 m
Time step	0.05 s
Time series length	660 s
Usable length of time series	630
Hub height	61 m
Grid Height	65 m
Grid Width	65 m
Vertical mean flow angle	8°
Turbulence Spectrum	Kaimal
IEC turbulence class	A

The grid point dimensions resulted in a 13×13 grid. We chose the dimensions based on previous experience with Germanischer Lloyd (GL) requirements; however NREL typically uses an 11×11 grid. The time step was chosen to give a valid bandwidth of 10 Hz, typical of measured data. The time series length was chosen to allow for a 30-second transient at the beginning of the simulation. The hub height was set at 61 meters because we were using a WindPACT 750 kW tower model. The vertical mean flow angle was based on IEC requirements (IEC-TC88 2005, Section 6.3). The Kaimal (1972) spectral model was used because it is one of the two IEC models (IEC-TC88 2005, Appendix B) available in TurbSim.

According to the IEC requirements, six 10-minute simulations per wind speed have to be run for the entire operating range. Due to time constraints, only two simulations per wind speed were run in the range of rated wind speed. Based on previous atmospheric testing experience, we expected that the highest loads would occur in this range.

Due to time constraints not all of the IEC extreme load cases were performed. We therefore simulated cases that were expected to be driving load cases in deflection for the flap/twist coupling concept according to Wetzel (2005) and Griffin (2004). The extreme loads were determined for the operating load cases, the extreme operating gust with direction change, and the extreme operating wind shear. Inputs for these load cases can be found in the IEC design requirements (IEC-TC88 2005). At the time of this writing, the extreme load cases for the 50-m rotor had not been performed.

RESULTS

For the results we will look at three different models, called STAR6, BASE6, and 50-m. These models, respectively, are the swept 56-m diameter rotor with 2.2 m of tip sweep, the same 56-m diameter rotor with no sweep, and a baseline rotor that is used on the Z-50 turbine. The details of the 50-m rotor are proprietary, so only normalized load values will be presented for this model.

Tip Twist

We first look at the twist behavior of the STAR rotor. Figure 3 below shows the tip twist versus 10-minute average wind speed. The 10-minute simulations were run with IECA turbulence. Two 10-minute simulations were run for each wind speed, each using a different random number generator seed. Negative tip twist is towards feather. At the top of the plot we observe twist of less than 1° for the straight rotors BASE6 and 50-m. The average tip twist for STAR6 reaches a minimum of -3° to -4° between 10 m/s and 11 m/s. The minimum values are approximately -5° for the full wind speed range.

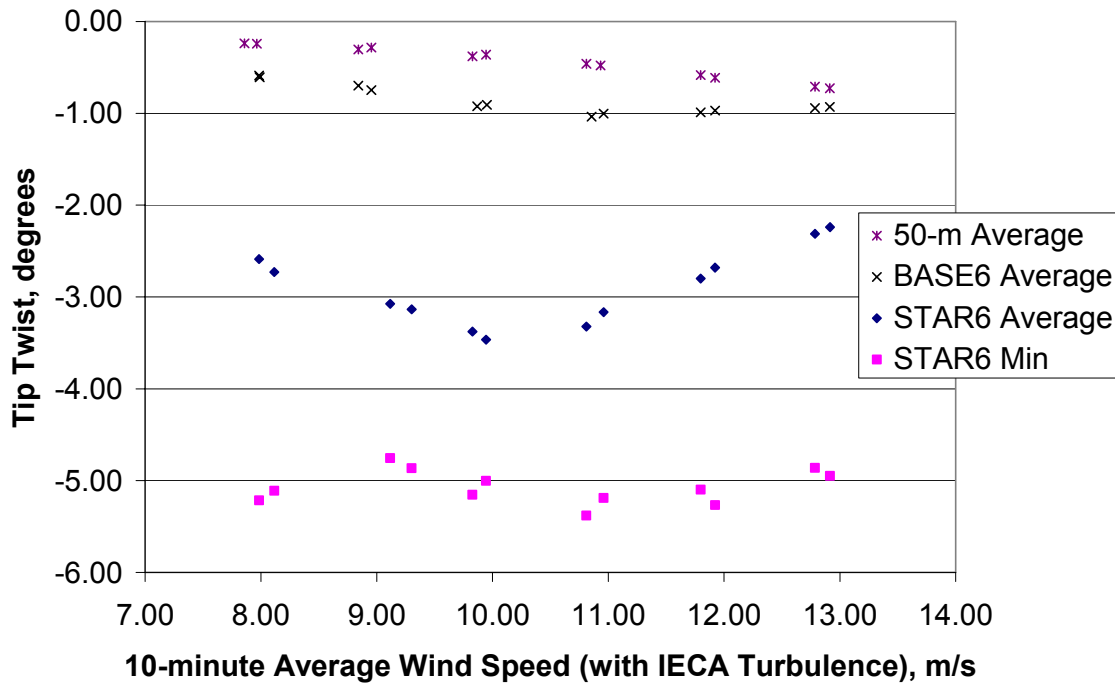


Figure 3. Tip twist for 10-minute turbulent simulations.

Root Flap Bending Moment

The blade root flap bending moment for the same conditions in Figure 3 is presented below in Figure 4. The moments are normalized to the maximum value obtained from the BASE6 simulation. The top three sets of data are the maximum values of the simulations, obtained from BASE6, STAR6 and 50-m in order of value respectively. The peak BASE6 value is approximately 20% higher than the peak STAR6 value, and 25% higher than the 50-m peak value. The average values are also shown, again in order as the maximum values. The peak average values for STAR6 and BASE6 occur between 10 m/s and 11 m/s. The peak average value for the 50-m model occurs between 11 m/s and 12 m/s.

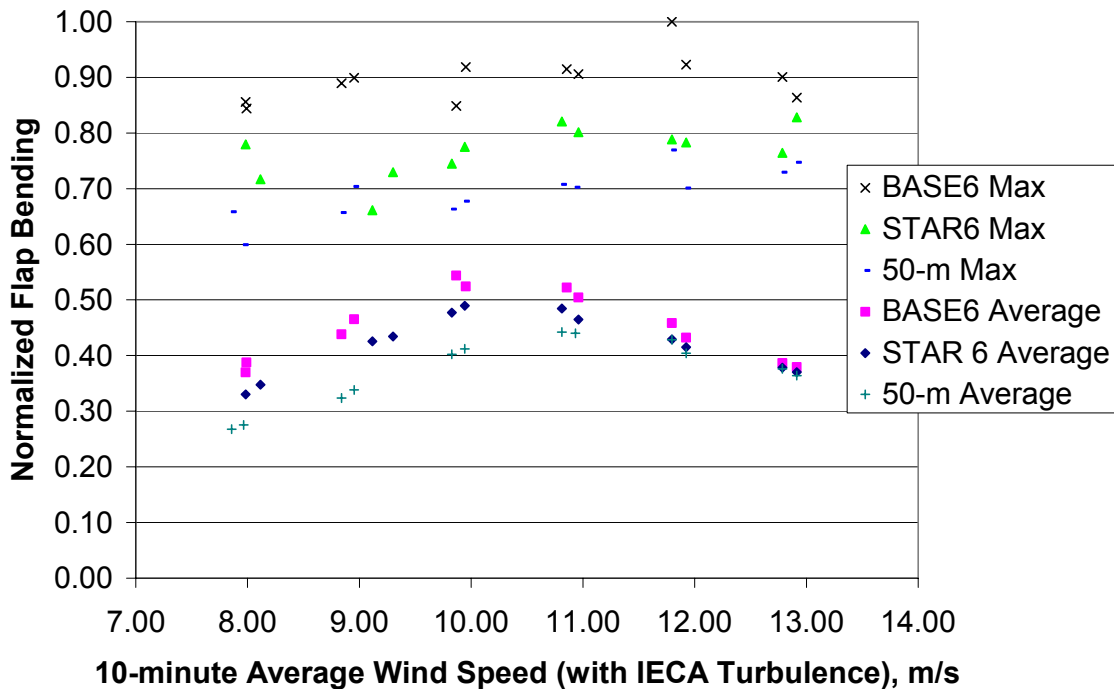


Figure 4. Blade root flap bending moment.

At this point in the design phase, we wished to optimize the geometry of the sweep for maximum load reduction. It was difficult to see improvements in plots such as Figure 4, so we plotted in Figure 5 the probability density of the flap bending moments for the 10 m/s simulation. The most right-hand side curve is for the BASE6. The next two curves to the left are for a later version of the STAR rotor with two different sweep curve exponents. The higher value represents more curvature outboard along the blade. The 50-m model was run at 11 m/s because we expected this to be the peak in flap loads for this model.

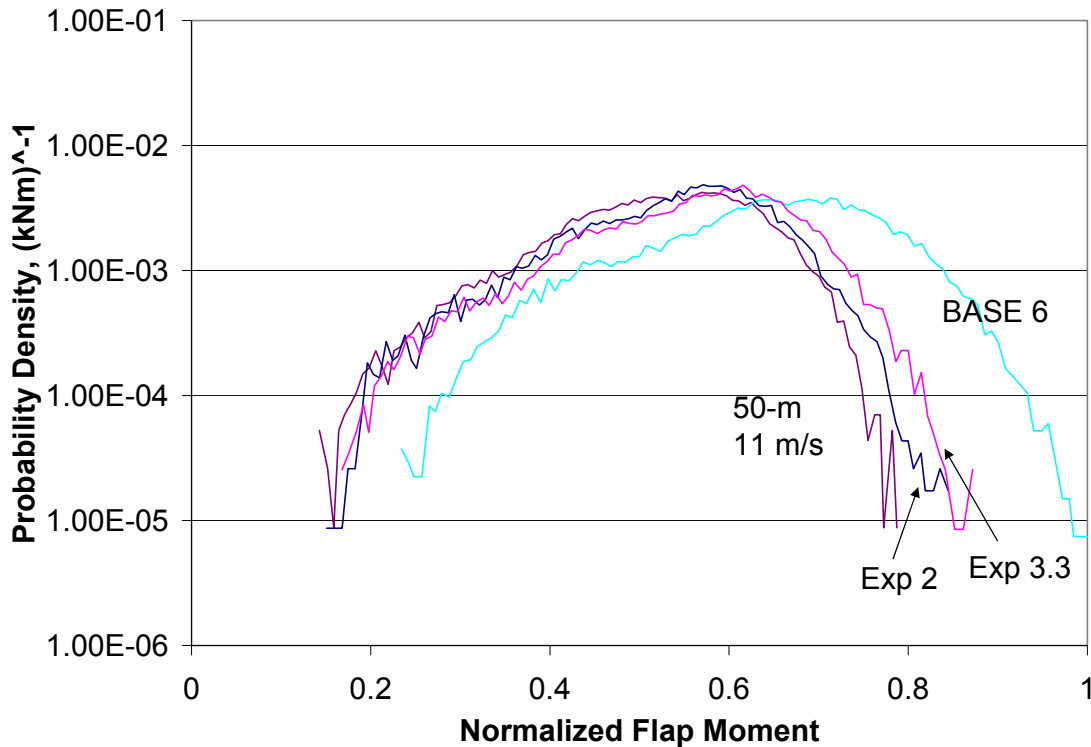


Figure 5. Histogram of flap bending moment for 10-minute 10 m/s turbulent simulation.

To show the relationship between root flap moment and blade tip twist, Figure 6 is presented below with time series data of tip twist, root flap, and blade pitch for a portion of a 10 m/s average simulation. This particular time series is for a later design of the STAR rotor that included more torsional flexibility. The tip twist is plotted positively for direct comparison to the root flap bending moment. The twist quite closely follows the flap moment, and can be seen to slightly lag as shown in the peak just prior to 200 s. After this peak the turbine pitches to control rotor speed.

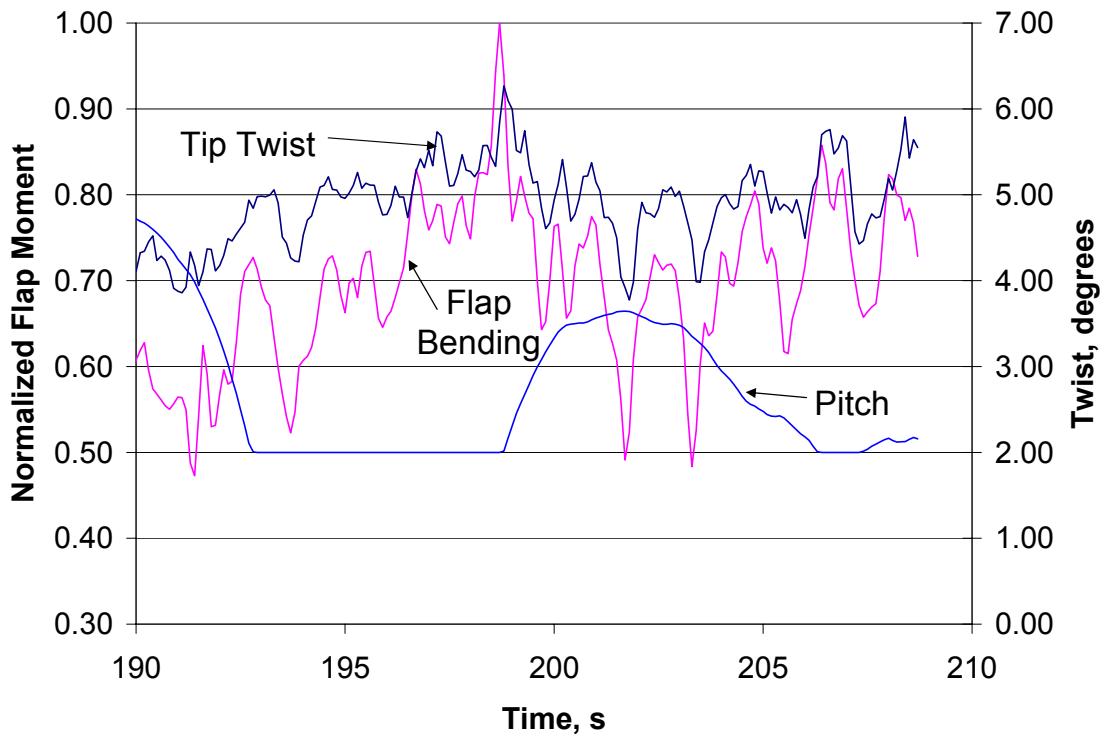


Figure 6. Time series of tip twist, flap bending, and blade pitch.

Deflection

The tip deflection of the models is presented below in Figure 7. The deflection values have been normalized to the available tower clearance. The maximum values for the simulations are shown, in order of BASE6, STAR6 and 50-m. The peak values for the STAR6 and the 50-m are roughly the same.

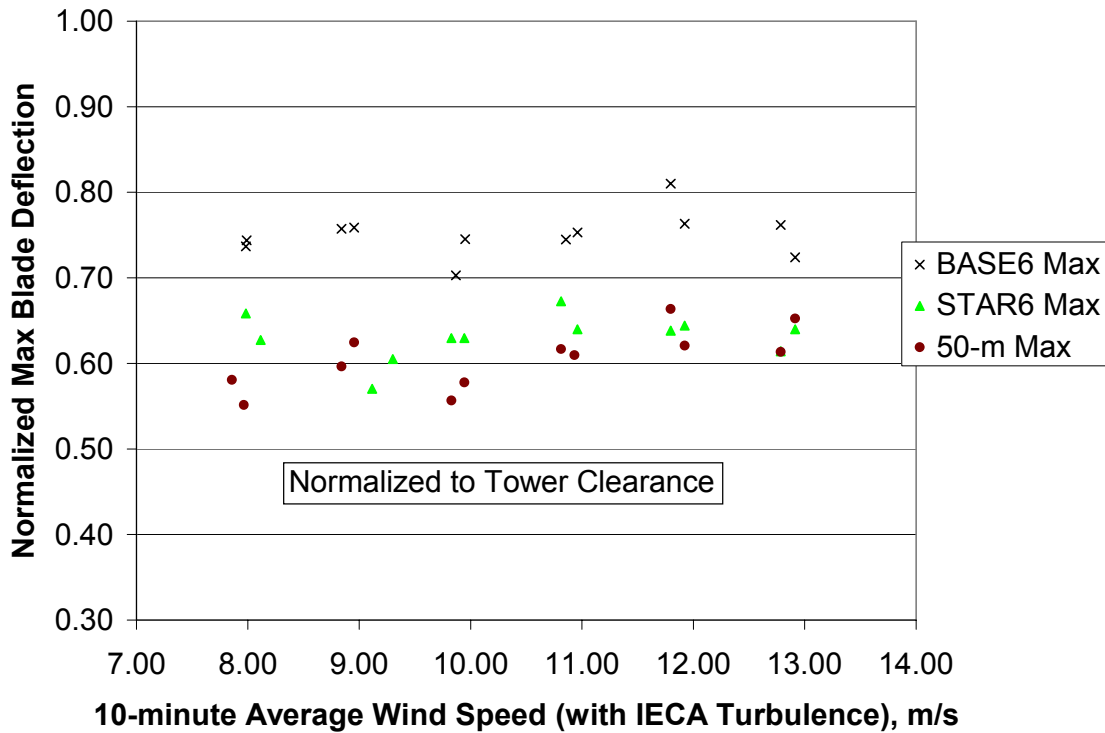


Figure 7. Normalized blade tip deflection.

Power

The 10-minute average generator power values are shown in Figure 8. The curves are ordered in value by BASE6, STAR6, and 50-m rotor. There is little variation between the values for BASE6 and STAR6, however there is a rough 100 kW difference between STAR6 and the 50-m power values below the rated wind speed for the simulated wind speeds.

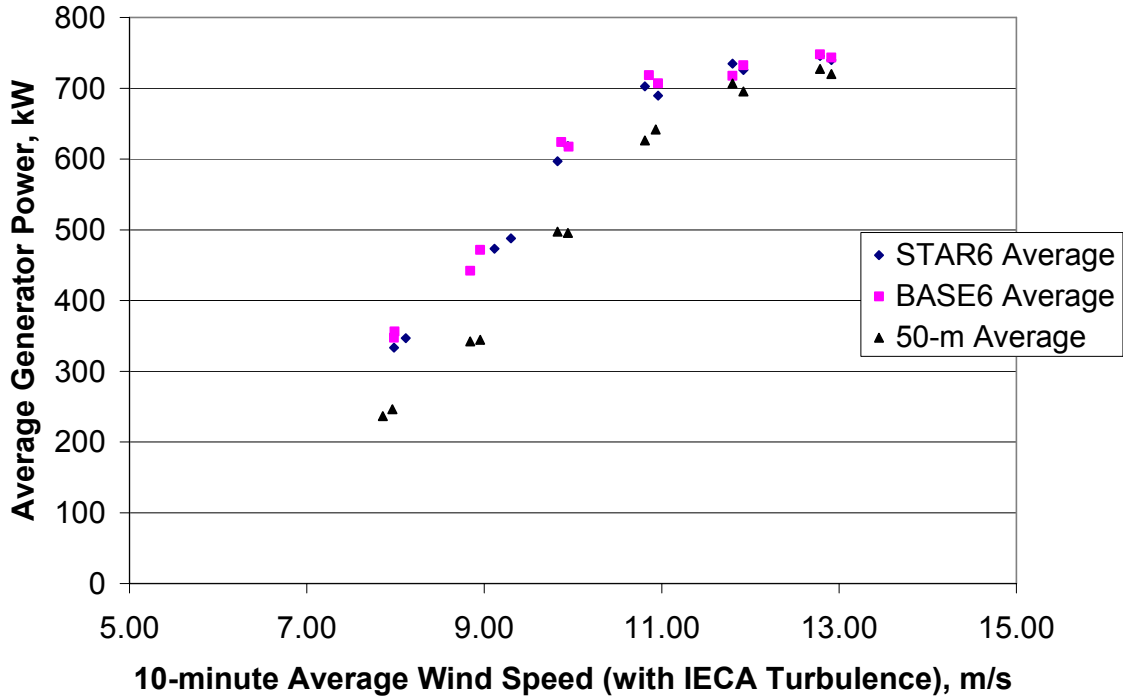


Figure 8. Power curves for the models.

Extreme loads

The results for extreme-load tip deflection are shown below in Table 2. The results are shown with and without safety factors included. The straight blade BASE6 exceeds the tower clearance for all conditions with safety factors included. For the STAR6, the deflection is at the limit with safety factors included for the extreme coherent gust with direction change.

Table 2. Extreme Load Blade Tip Deflections

Load Case	Model	Normalized Tip Deflection	With Safety Factor
Power Production	BASE6	0.81	1.20
	STAR6	0.67	0.99
Extreme Coherent Gust with Direction Change	BASE6	0.76	1.13
	STAR6	0.67	1.00
Extreme Wind Shear	BASE6	0.72	1.07
	STAR6	0.61	0.92

DISCUSSION

The authors caution that the results presented are based on modeling and have not been validated with atmospheric testing results. Atmospheric testing of the swept rotor is intended to begin in the winter of 2006-2007.

The ADAMS models show that the STAR6 blade is twisting towards feather as expected. The peak average value falls between 10 m/s and 11 m/s (Figure 3). This is the same wind speed range for the peak flap bending loads, and is typical of peak loads in the “knee” of the power curve (Figure 8). Twist is shown to be highly dynamic (Figure 6) and closely follows the flap bending loads. No stability problems or erratic behavior are observed in the blade pitch control. The peak twist is on the order of 5°, which is on the low end of the design range. We have since designed the blade with more twist response.

For flap bending (Figure 4), there is a substantial reduction in peak load with sweep. However, the STAR6 peak is slightly higher than the 50-m baseline. Plotting of flap bending probability density functions (Figure 5) can be used to determine optimum geometry for load reduction of the swept planform.

It is interesting to note in the tip deflection results (Figure 7) that even though the sweep concept requires the blade to deflect towards the tower to induce twist, the reduction in loads is such that the overall peak tip-deflection is of the same level as the baseline turbine.

The power results in Figure 8 are surprising because there seems to be little loss in power due to the combined effect of sweep and twist to feather compared to a straight blade

design. The difference in below rated power between the STAR6 and the 50-m rotor suggests that the expected increase in annual energy capture will meet the design goals.

For the STAR6, the worst case condition is the extreme coherent gust with direction change (Table 2), where the deflection is at the limit of tower clearance with safety factors included. We note that upwind coning can be used to increase the tower clearance; however this is at the expense of increased flap bending loads.

As stated above, we have not included the drivetrain and tower degrees of freedom in the dynamic modeling. Future work will be required to include these models by incorporating frequencies obtained from field test results. The full system model will allow for any dynamic resonances to be uncovered. We also intend to determine the flutter boundary of this concept, using methods developed by Lobitz (2004). The increased torsional flexibility of the design increases the probability of flutter; however, aft tip-sweep should act to increase the flutter stability. Also, no flutter behavior has been observed in the operating simulations. We also need to complete the full suite of IEC loads cases to verify that we are within the load envelope of the Z-50 turbine.

For future work, we also intend to enhance the capability of FAST to include the blade sweep geometry and twist degrees of freedom. This has the potential to allow for automated design optimization and load case runs at minimal cost.

CONCLUSIONS

For the Knight & Carver LWST contract, a dynamic analysis of a swept-blade wind turbine rotor has been developed. The rotor is intended to be tested on a Zond Z-50 750 kW turbine, and the swept blade is expected to increase energy capture by 5% to 10% without increasing the load envelope. The blade model, the STAR6, had 28 m in length and has 2.2 m of tip sweep. NREL's FAST code was used as a pre-processor for ADAMS simulations of the turbine. A straight-bladed turbine model of the same geometry and a baseline 50-m diameter rotor were also modeled for comparison. Key results of modeling effort were as follows:

- Peak twist of the STAR6 was 5°, which was at the low end of the design range
- The twist was highly dynamic and followed the flap bending loads
- Peak flap bending for the STAR6 was reduced by 20% compared to the straight blade; however the loads were slightly higher than the 50-m baseline rotor.
- Optimization of the sweep geometry for lowest loads was obtained by plotting the probability density of the flap bending loads.
- Blade deflection of the STAR6 was on the same level as the 50-m baseline for operating simulations.
- Peak extreme deflection for the STAR6 was obtained with the extreme coherent gust with direction change
- Power capture for the STAR6 shows little detriment compared to the straight-bladed rotor, and average capture is expected to be as much as 5% to 10% over the 50-m rotor.

Future modeling work will include tower and drivetrain modeling of the turbine, and we intend to add sweep geometry and twist degrees of freedom to the FAST code.

REFERENCES

Althaus, D. (1986). *Niedriggeschwindigkeitsprofile*, Braunschweig, Germany, Vieweg.

Buhl Jr, M. L. (2005, 20 June 2005). NWTC Design Codes (WT_Perf) [online]. Available: <http://wind.nrel.gov/designcodes/simulators/wtperf/>.

Fingersh, L. J. and P. W. Carlin (1998). "Results from the NREL Variable-Speed Test Bed." *A Collection of the 1998 ASME Wind Energy Symposium Technical Papers at the 36th AIAA Aerospace Sciences Meeting and Exhibit, Reno, NV, 12-15 January 1998*. AIAA/ASME; pp. 233-237.

Griffin, D. A., M. Zuteck, et al. (2004). "Development of Prototype Carbon-Fiberglass Wind Turbine Blades: Conventional and Twist-Coupled Designs." *2004 ASME Wind Energy Symposium, Reno, NV, 5-8 January 2004*. American Society of Mechanical Engineers; pp. 1-12.

Hand, M. M. (1999). *Variable-Speed Wind Turbine Controller Systematic Design Methodology: A Comparison of Non-Linear and Linear Model-Based Designs*. Golden, CO; National Renewable Energy Laboratory. NREL/TP-500-25540. 117 p.

Hoerner, S. F. (1985). *Fluid-Dynamic Lift*, Published by Liselotte A. Hoerner.

IEC-TC88 (2005). *Wind turbines - Part 1: Design Requirements (Final Draft)*. Geneva, Switzerland; International Electrotechnical Commission. IEC 61400-1 Ed. 3 (88/228/FDIS). 92 p.

Jonkman, J. M. (2005, 2 August 2005). NWTC Design Codes (FAST) [online]. Available: <http://wind.nrel.gov/designcodes/simulators/fast/>.

Jonkman, J. M. and M. L. Buhl Jr (2004). "New developments for the NWTC's fast aeroelastic HAWT simulator." *2004 ASME Wind Energy Symposium, Reno, NV, 5-8 January 2004*. AIAA/ASME; pp. 181-191.

Kaimal, J. C., J. C. Wyngaard, et al. (1972). "Spectral characteristics of surface-layer turbulence." *Quarterly Journal of the Royal Meteorological Society* **98**: pp. 563-589.

Kelley, N. D. and B. J. Jonkman (2005, 20 June 2005). NWTC Design Codes (TurbSim) [online]. Available: <http://wind.nrel.gov/designcodes/preprocessors/turbsim/>.

Laino, D. J. (2005a, 20 September 2005). NWTC Design Codes (IECWind) [online]. Available: <http://wind.nrel.gov/designcodes/preprocessors/iecwind/>.

Laino, D. J. (2005b, 17 May 2005). NWTC Design Codes (YawDyn) [online]. Available: <http://wind.nrel.gov/designcodes/simulators/yawdyn/>.

Liebst, B. S. (1986). "Wind Turbine Gust Load Alleviation Utilizing Curved Blades." *Journal of Propulsion* 2(4): pp. 371-377.

Lobitz, D. W. (2004). "Aeroelastic Stability Predictions for a MW-sized Blade." *Wind Energy* 7: pp. 211-224.

Lobitz, D. W., P. S. Veers, et al. (1996). "Enhanced Performance of HAWTs Using Adaptive Blades." *Wind Energy '96, Energy Week Conference & Exhibition Book VIII Volume 1, Houston, TX, 29 January-2 February 1996*. PennWell Conferences & Exhibitions; pp. 41-45.

Wetzel, K. K. (2005). "Utility Scale Twist-Flap Coupled Blade Design." *2005 ASME Wind Energy Symposium; 10-13 January 2005; Reno, NV*. AIAA/ASME; pp. 382-394.

Zuteck, M. (2002). *Adaptive Blade Concept Assessment: Curved Planform Induced Twist Investigation*. Albuquerque, NM; Sandia National Laboratories. SAND2002-2996. 24 p.